

What Determines Inhomogeneous Line Widths in Semiconductor Microcavities?

D. M. Whittaker

Toshiba Cambridge Research Centre, 260 Cambridge Science Park, Milton Road, Cambridge CB4 4WE. United Kingdom

Microcavity inhomogeneous line widths are calculated numerically using a microscopic two dimensional model of the polariton interaction with quantum well disorder. The calculations show that in most structures the line widths are determined by disorder scattering between polariton and exciton states. This is because motional narrowing effectively removes the contribution due to multiple scattering between polariton states.

Recent experimental results [1] have shown the importance of motional narrowing in determining the line widths of features in the reflectivity spectra of semiconductor microcavities. In a microcavity, the fundamental optical excitations are polaritons, arising from the coupling of a confined cavity photon mode to exciton states in quantum wells within the cavity. The spectral features associated with the polariton are broadened, both homogeneously due to the finite life time of the cavity photon, and inhomogeneously due to the interaction with disorder in the quantum wells. Motional narrowing occurs because the polaritons, being part photon, have very long wavelengths compared with those typical for excitons. The inhomogeneous broadening is therefore substantially reduced by averaging over a large area of the much shorter length scale disorder potential.

The important physical parameters which determine the inhomogeneous line widths are the dispersions of the exciton and photon, the strength of their interaction, and the statistical properties of the disorder. A good approximation is to treat each dispersion as parabolic, the photon mass, $M_l \sim 3 \times 10^{-5} m_e$, being a consequence of the effects of cavity confinement [2]. The exciton-photon coupling leads to the formation of two polariton branches, separated at resonance by the vacuum Rabi splitting, $\hbar\Omega \sim 5$ meV, which provides a measure of the strength of the interaction. Finally, the quantum well disorder potential is characterised by its amplitude V_0 , of order a few meV, and a correlation length $l_c \sim 100$ Å.

The original treatment of motional narrowing in Ref. [1] assumed the weak disorder limit, $V_0 \ll \hbar\Omega$, in which only scattering between low momentum polariton states on the same branch is allowed. It was then possible to use a simple scaling argument to predict the variation of the line widths with detuning. However, in a comment on that model, Agranovich et al. [3] showed that the same scaling argument predicts the actual value of the inhomogeneous line width, at resonance, to be

$$\Gamma_{2d} \sim \frac{1}{2} V_0^2 \left(\frac{\hbar^2}{2M_l l_c^2} \right)^{-1}. \quad (1)$$

For physically reasonable parameters, Γ_{2d} is extremely small, $\sim 10^{-4}$ meV, compared with the experimental inhomogeneous line widths of about 0.3 meV.

The main aim of this letter is to demonstrate that, besides the polariton multiple scattering processes which give Eq.(1), there is a contribution to the line width due

to disorder scattering between polariton and higher momentum exciton states. Such scattering is not included in the scaling treatment, since it assumes the polariton dispersion is parabolic, while in fact the two branches decouple at large wave-vectors. The more realistic calculation described here uses a numerical simulation of a polariton in the presence of the disorder, which automatically includes both types of scattering. However, in a typical structure, the small value of the polariton multiple scattering contribution, estimated above, means that polariton to exciton scattering processes dominate. On the other hand, in a high quality sample, where $V_0 < \Omega/2$, scattering of polaritons into exciton states becomes energetically impossible, and only the small polariton multiple scattering contribution remains.

The numerical model used here is physically similar, though solved differently, to the one dimensional simulations of Savona *et al.* [4]. However, motional narrowing in one dimension is significantly less important than in two, because averaging over a 1d strip samples much less of the variation of the potential than an average over a 2d area of equivalent size. This difference can be seen very clearly by calculating the 1d equivalent of Eq.(1), for the contribution of polariton multiple scattering to the line width,

$$\Gamma_{1d} \sim \frac{1}{2} V_0^{4/3} \left(\frac{\hbar^2}{2M_l l_c^2} \right)^{-1/3} \quad (2)$$

For the parameters that gave $\Gamma_{2d} \sim 10^{-4}$ meV, $\Gamma_{1d} \sim 10^{-1}$ meV, three orders of magnitude greater, and far more comparable to the experimental line widths. This comparison suggests that the balance between polariton multiple scattering and polariton to exciton scattering should be very different in such 1d calculations when compared to real 2d structures.

The numerical treatment is based on the two level model of the polariton, in which a discrete cavity mode couples to the exciton ground state. The exciton interacts with the quantum well disorder potential, so in-plane momentum is not conserved. Thus the model consists of coupled two dimensional partial differential equations describing the in-plane motion of both the exciton and cavity photon. This model contains a number of approximations, most notably the omission of excited exciton states and the lack of a proper treatment of the effects of the magnetic field applied in the experiments. These approximations restrict the possibilities for precise comparisons with experiment, but the the good general agree-

ment which is obtained suggests that the essential physics is included.

The Hamiltonian for the model system takes the form

$$H = \begin{pmatrix} -\frac{\hbar^2}{2M_l}\nabla^2 + \delta - i\gamma & \hbar\Omega/2 \\ \hbar\Omega/2 & -\frac{\hbar^2}{2M_e}\nabla^2 + V(\mathbf{r}) \end{pmatrix} \quad (3)$$

In addition to the photon mass M_l , and the vacuum Rabi splitting, $\hbar\Omega$, discussed above, M_e is the exciton mass, δ the detuning of the cavity photon relative to the exciton, and γ , the photon homogeneous width (due to escape through the mirrors). The quantum well disorder, $V(\mathbf{r})$, is a Gaussian stochastic potential, constructed in the Fourier domain, following the method described by Glutsch et al. [5]. Its amplitude, V_0 , is defined as the width at half maximum of the potential probability distribution.

The inhomogeneously broadened spectra are calculated from the photon Green's function

$$G_k(t) = -i \langle \mu_k | e^{-iHt/\hbar} | \mu_k \rangle \theta(t) \quad (4)$$

where $|\mu_k\rangle$ represents a state of the system (not an eigenstate) consisting of a plane wave cavity photon with in-plane wavevector k and no exciton. All the results given in this letter are for normal incidence, corresponding to $k = 0$. The Green's function describes how a photon which enters the cavity is scattered out of its initial plane wave state by interactions with the disordered exciton. The plotted spectra are actually the photon spectral functions, obtained by Fourier transforming the Green's function to give $\tilde{G}_k(\omega)$ and extracting the imaginary part. They correspond to what would be seen in an absorption measurement, but the line widths should be the same in reflectivity experiments.

The Green's function is obtained using an approach similar to that of Glutsch et al. [5]. Starting from an initial state $|\psi(0)\rangle = |\mu_k\rangle$, the wavefunction $|\psi(t)\rangle$ is calculated by numerically solving the time dependent Schrödinger equation using the Hamiltonian Eq.(3). From the solution at each time t , $G_k(t)$ is found by evaluating $\langle \mu_k | \psi(t) \rangle = \langle \mu_k | e^{-iHt/\hbar} | \mu_k \rangle$. The calculation is carried out on a two dimensional spatial grid, using a standard alternating direction Crank-Nicholson algorithm [6]. The main difficulty is the need to use a grid which is fine enough to reveal the correlated structure of the potential, on a length scale $l_c \sim 100 \text{ \AA}$, yet large enough to avoid significant size quantisation for the low mass photon states. The present numerical results are for a $2^{11} \times 2^{11}$ grid with spacing 100 \AA , giving photon quantisation energies $\sim 0.05 \text{ meV}$, considerably smaller than typical calculated line widths of $\sim 0.3 \text{ meV}$.

Fig.1 shows spectra calculated for a realistic set of parameters: $M_l = 3 \times 10^{-5}m_e$, $M_e = 0.5m_e$, $\hbar\Omega = 5 \text{ meV}$, $V_0 = 3.5 \text{ meV}$ and $l_c = 100\text{\AA}$. For clarity, the photon homogeneous line width, γ , has been set to zero. The spectra display the variations in intensity typical of an anti-crossing between two states, only one of which, the photon, has intrinsic strength. Close to resonance, where the

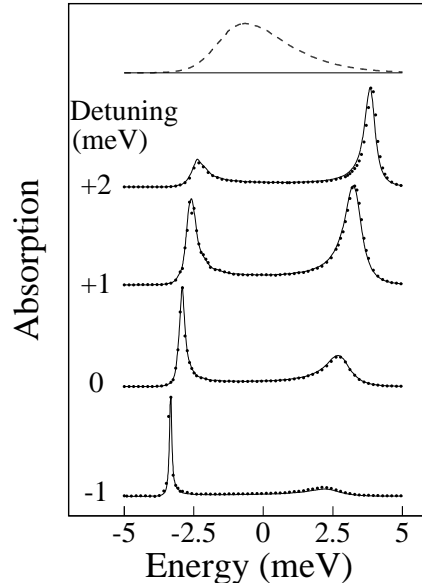


FIG. 1. Numerical absorption spectra (dots) at various values of the detuning δ . The dashed curve shows the bare exciton lineshape. The solid lines are the predictions of the coupled oscillator model (see text).

polariton branches are equal mixtures of photon and exciton, the two peaks have similar integrated strength. Further away from resonance, the more photon-like peak is strong, while the other, predominantly exciton, is weak. The figure also shows the bare exciton spectrum, which is asymmetrically broadened because of the finite exciton mass [7,8].

In Fig.2, the line widths measured from the spectra are plotted as a function of detuning. The asymmetry between the line widths of the two branches at zero detuning is very apparent: the upper branch has a width of $\sim 1 \text{ meV}$, and the lower branch 0.25 meV . When a realistic photon homogeneous broadening of $\gamma = 1.25 \text{ meV}$ is included in the calculation, the widths become 1.4 and 0.6 meV respectively, close to the experimental values of ~ 1.5 and 0.75 meV found in Ref. [1]. However, because of the lack of a proper treatment of the magnetic field used in the experiments, this agreement can only be regarded as suggestive.

The solid lines in Figs.1-2 show the results of a simpler model, which provides an excellent fit to the numerical data. In this model, the full exciton Green's function $\tilde{G}_{kk'}^e(\omega)$ is approximated by its diagonal part $\delta_{kk'}\tilde{G}_k^e(\omega)$. With k thus conserved, the polariton problem simplifies to a pair of coupled oscillators, which is easily solved to obtain the polariton Green's function

$$\tilde{G}_k(\omega) = \frac{1}{\hbar\omega + i\gamma - \delta_k - (\hbar\Omega/2)^2 \tilde{G}_k^e(\omega)} \quad (5)$$

where $\delta_k = \delta + \hbar^2 k^2 / (2M_l)$ is the detuning for wavevector k . The bare exciton Green's functions, $\tilde{G}_k^e(\omega)$ are

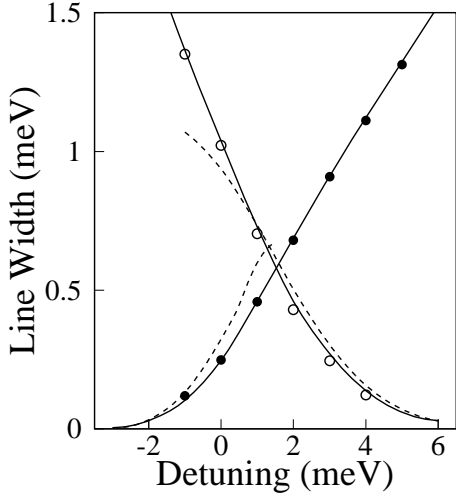


FIG. 2. Numerical line widths as a function of detuning, δ , for upper (open symbols) and lower (filled symbols) polaritons. The solid lines are the predictions of the coupled oscillator model, the dashed lines those of the absorption model.

calculated using the same type of numerical simulation as for the full polariton. However approximate expressions for the finite mass exciton spectral function, by Glutsch and Bechstedt [8], could be used for large exciton masses.

Eq.(5) excludes polariton multiple scattering, since the polariton always has a definite wave-vector, k . However, polariton to exciton scattering processes are included, because the exciton Green's function $\tilde{G}_k^e(\omega)$ takes care of the multiple scattering of excitons between different momentum states. It has a finite imaginary self energy determining the rate at which excitons scatter out of the state with wave-vector k . The good fit to the numerical data which is obtained indicates that the contribution of polariton multiple scattering is negligible for these parameters, as the estimate of Eq.(1) suggests.

In the coupled oscillator model, the difference between the widths of the two polariton branches is a consequence of the asymmetry of the exciton line shape, which is, in turn, a result of the finite exciton mass. On the low energy side of the line, there is an exponential cut-off, reflecting the distribution of minima in the disorder potential, while on the high energy side the strength falls off more slowly, as $\sim \omega^{-2}$, determined by the perturbation of higher momentum plane wave states by the potential [10]. This explanation for the asymmetry is thus similar in essence to the suggestion by Savona *et al* [4] that the larger upper branch width is caused by scattering into higher momentum exciton states.

An approximate expression for the polariton line widths can be found by examining Eq.(5). For sufficiently small broadening, the polariton lineshape approximates to a Lorentzian, with full width Γ dependent on the imaginary part of the denominator at the polariton energy, ω_p , according to

$$\Gamma = 2|c_l|^2 \left(\gamma - \Omega^2/4 \text{Im}\{\tilde{G}_k^e(\omega_p)\} \right) \quad (6)$$

where $|c_l|^2$ is the photon fraction of the polariton. This approximation is shown as the dashed lines on Fig.2. For large photon fractions, when the polaritons are resonant with the tails of the exciton line (see Fig.1), the approximate expression agrees fairly well with the exact curve. However, when $|c_l|^2$ becomes small, Eq.(6) predicts $\Gamma \rightarrow 0$, while the true value tends to the exciton line width. This behaviour can be understood more physically by noting that the second term in Eq.(6) describes homogeneous broadening of the polariton due to the loss of photons in the cavity by absorption into exciton states – it is proportional to the photon fraction and the exciton absorption strength $-\text{Im}\{\tilde{G}_k^e(\omega_p)\}$. This is to be expected for a state in the tail of the exciton line shape, which is too weak to require a strong coupling treatment, and thus acts simply as a source of absorption, like the continuum states without a magnetic field [9]. The absorption picture breaks down when the polariton is resonant with the states near the centre of the exciton line, and the full strong coupling treatment is required.

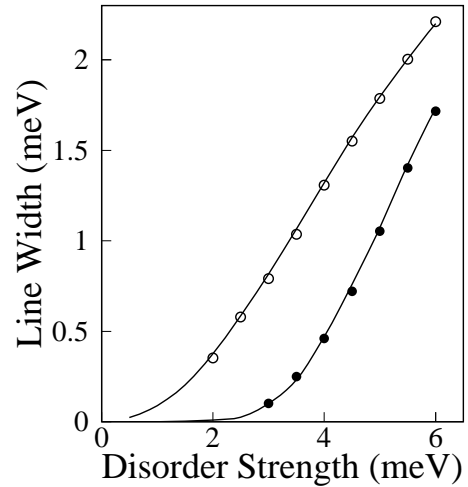


FIG. 3. Numerical line widths as a function of disorder strength, V_0 , for upper (open symbols) and lower (filled symbols) polaritons. The solid lines are the predictions of the coupled oscillator model.

The coupled oscillator model described above can be shown to be a generalisation of the phenomenological treatment of a translationally invariant Gaussian broadened exciton, proposed by Houdré *et al* [11]. The main improvement is that the Gaussian exciton line is replaced by an asymmetric form because of the finite exciton mass. More importantly, the present work demonstrates that motional narrowing is the reason why such a model succeeds, in that it eliminates the polariton multiple scattering contribution to the line width.

The most intriguing feature of the Gaussian model, discussed by Savona and Weisbuch [12], is the prediction

that the disorder contribution to the line width should disappear in high quality structures when polariton to exciton scattering becomes impossible. In terms of the absorption picture, this happens when the polariton states are so far into the tails of the exciton line that no absorption occurs. The present calculations support this prediction, as is shown by Fig.3, where numerical and coupled oscillator model line widths are plotted as a function of disorder strength, V_0 . As in Ref. [12], the lower branch width rapidly becomes very small when $V_0 < \Omega/2$. The effect is much less pronounced for the upper branch, because of the longer tail on the high energy side of the finite mass exciton line shape.

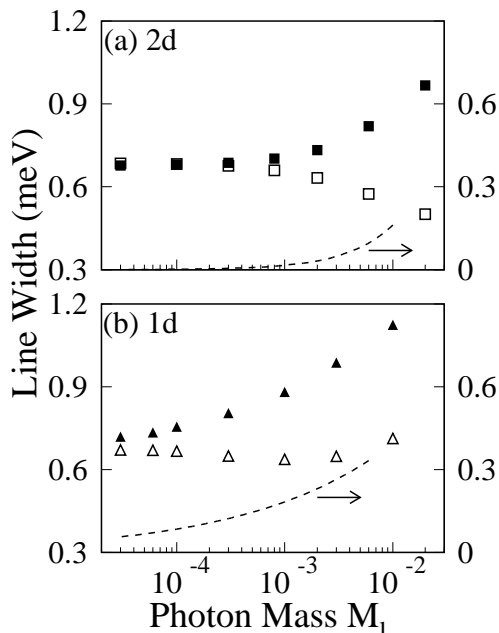


FIG. 4. Numerical line widths as a function of photon mass, M_l , for upper (open symbols) and lower (filled symbols) polaritons in (a) two dimensions and (b) one dimension, with $M_e \rightarrow \infty$. Also shown (dashed lines and right hand scale) are the polariton multiple scattering expressions, Γ_{2d} and Γ_{1d} of Eqs. (1) and (2).

All the numerical data in Figs.1-3 are very well explained by the coupled oscillator model, which includes only polariton to exciton scattering. It is not possible in the numerical calculations to resolve directly the very small polariton multiple scattering term, Γ_{2d} from Eq.(1), even for $V_0 \ll \Omega/2$, when it should be the only contribution to the line width. However, indirect evidence for the existence of the process can be obtained by considering non-physical situations in which polariton multiple scattering is more important. As an example, Fig.4(a) shows the dependence on the photon mass, M_l , of the numerically simulated line widths at resonance. The oscillator model predicts that the line widths of the two branches should be equal, as the calculation is for infinite exciton mass, and independent of M_l . For the real $M_l = 3 \times 10^{-5} m_e$, the line widths are indeed equal.

However, when M_l is significantly increased a difference appears, which is clearly due to polariton multiple scattering, as it grows in proportion to Γ_{2d} , plotted as the dashed curve on the figure. Fig.4(b) shows similar data for a one dimensional system. Again, the difference between the upper and lower branch widths grows, for small M_l , in proportion to Γ_{1d} [13]. However, because motional narrowing is much less effective in 1d than 2d, even for the real $M_l = 3 \times 10^{-5} m_e$, there is a measurable difference in line widths, some 0.05 meV. This result emphasises that there are significant differences between the scattering processes which occur in 1d and 2d systems.

In summary, the numerical simulations presented in this letter have shown that there are two types of processes by which disorder contributes to the broadening of microcavity line widths. In typical structures, scattering between photon and exciton states dominates. From the point of view of the photon, this is just a form of life time broadening, caused by absorption into states in the tails of the exciton distribution, and is thus in some senses homogeneous. The true inhomogeneous width, the result of multiple scattering of polaritons by the disorder, is extremely small because of motional narrowing. However, it should be the only disorder contribution to the width of the lower polariton branch in high quality structures.

I would like to thank C. L. Foden, M. S. Skolnick and J. J. Baumberg for their helpful comments on this work.

-
- [1] D. M. Whittaker, P. Kinsler, T. A. Fisher, M. S. Skolnick, A. Armitage, A. M. Afshar, M. D. Sturge and J. S. Roberts, Phys. Rev. Lett. **77**, 4792 (1996).
 - [2] R. Houdré, C. Weisbuch, R. P. Stanley, U. Oesterle, P. Pellandini and M. Ilegems, Phys. Rev. Lett. **73**, 2043 (1994).
 - [3] V. M. Agranovich, G. C. La Rocca and F. Bassani, Comment submitted to Phys. Rev. Lett.
 - [4] V. Savona, C. Piermarocchi, A. Quattropani, F. Tassone and P. Schwendimann, Phys. Rev. Lett. **78**, 4470 (1997).
 - [5] S. Glutsch, D. S. Chemla and F. Bechstedt, Phys. Rev. B **54**, 11592 (1996).
 - [6] W. H. Press, S. A. Teukolsky, W. T. Wetterling and B. P. Flannery in *Numerical Recipes in Fortran*, 2nd Edition (Cambridge University Press, 1992) pp 838-848.
 - [7] R. F. Schnabel, R. Zimmermann, D. Bimberg, H. Nickel, R. Lösch and W. Schlapp, Phys. Rev. B **46**, 9873 (1992).
 - [8] S. Glutsch and F. Bechstedt, Phys. Rev. B **50**, 7733 (1994).
 - [9] J. Tignon, P. Voisin, C. Delalande, M. Voos, R. Houdré, U. Oesterle and R. P. Stanley, Phys. Rev. Lett. **74**, 3967 (1995).
 - [10] Al. L. Efros, C. Wetzel and J. M. Worlock, Il Nuovo Cimento **17 D**, 1447 (1995).
 - [11] R. Houdré, R. P. Stanley and M. Ilegems, Phys. Rev. A **53**, 2711 (1996).
 - [12] V. Savona and C. Weisbuch, Phys. Rev. B **54**, 10835 (1996).
 - [13] The plotted width is actually half of Γ_{1d} in Eq. (2), as this fits better to calculated exciton line widths in 1d.